



Subsidence map for the west part of Tokyo Bay shore area liquefied in the March 11th, Great East Japan Earthquake

K. Kajihara⁽¹⁾, K. Konagai⁽²⁾, T. Kiyota⁽³⁾, S. Shibuya⁽⁴⁾ and I. Sato⁽⁵⁾

⁽¹⁾ Student, Graduate school of Urban Innovation, Yokohama National University, Japan, kajihara-kazuhiro-hc@ynu.jp

⁽²⁾ Professor, Institute of Urban Innovation, Yokohama National University, Japan, konagai@ynu.ac.jp

⁽³⁾ Associate Professor, Institute of Industrial Science, the University of Tokyo, kiyota@iis.u-tokyo.ac.jp

⁽⁴⁾ Aero Asahi Corp., Japan, kenichi-shibuya@aeroasahi.co.jp

⁽⁵⁾ Aero Asahi Corp., Japan, isao-satou@aeroasahi.co.jp

Abstract

The Great East Japan Earthquake of March 11th, 2011 (Mw=9.0) caused severe liquefaction damage over the entire stretch of reclaimed lands along the coast of the Tokyo Bay. In response to this earthquake, liquefaction-induced ground subsidence map for the eastern part of Tokyo Bay Shore area was immediately prepared by comparing a set of the Digital Surface Models (DSMs) before (2006) and after (2014) the earthquake, and subtracting tectonic displacements. This soil subsidence map is further extended herein to cover the Keihin-Industrialized region that encompasses the metropolis of Tokyo and includes a coastal part of Kanagawa prefecture. The obtained map describes in detail the spatial distribution of the earthquake-induced soil subsidence in this large industrial belt along the northwestern shore of Tokyo Bay.

Keywords: Great East Japan Earthquake; Soil subsidence; Tokyo Bay shore area

1. Introduction

Tokyo Bay area is one of the most urbanized areas in Japan with millions inhabitants and the ports/factories to support metropolitan activities. On March 11th, 2011, a gigantic earthquake of moment magnitude Mw 9.0 occurred off the Pacific coast of Tohoku, Honsyu Island, Japan. This earthquake is officially named “The 2011 Off the Pacific Coast of Tohoku Earthquake”, which is commonly known as the “Great East Japan Earthquake”. The Great East Japan Earthquake caused severe soil liquefaction over the entire stretch of reclaimed lands along the coast of Tokyo Bay, which is located about 350 kilometers away from the epicenter of this earthquake. The liquefied areas along the coast of Tokyo Bay reportedly reached 42 km² [1].

Major problems associated with liquefaction are ground subsidence, tilting of houses, buckling of roads, lifelines cutting, etc. In addition, what we should not forget is that liquefaction can recur at the same locations. Wakamatsu has confirmed that sand deposits, which were once liquefied in past earthquakes, did liquefy again in the Great East Japan earthquake at 145 locations in both Kanto and Tohoku Regions in Japan. Taking into account the high risk of re-liquefaction, it is very important for relevant organization to have quantitative information of the soil subsidence to be prepared for future earthquakes.

In response to this earthquake, liquefaction-induced ground subsidence map for the eastern part of the Tokyo Bay Shore area was immediately prepared by comparing a set of the Digital Surface Models (DSMs) before (2006) and after (2014) the earthquake, and subtracting tectonic displacements [2].

Soil subsidence map is further extended herein to cover the Keihin-Industrialized region that encompasses the metropolis of Tokyo and the eastern part of Kanagawa prefecture. The obtained map describes in detail the spatial distribution of the earthquake-induced soil subsidence in this large industrial belt along the northwestern shore of Tokyo Bay (Fig.1).

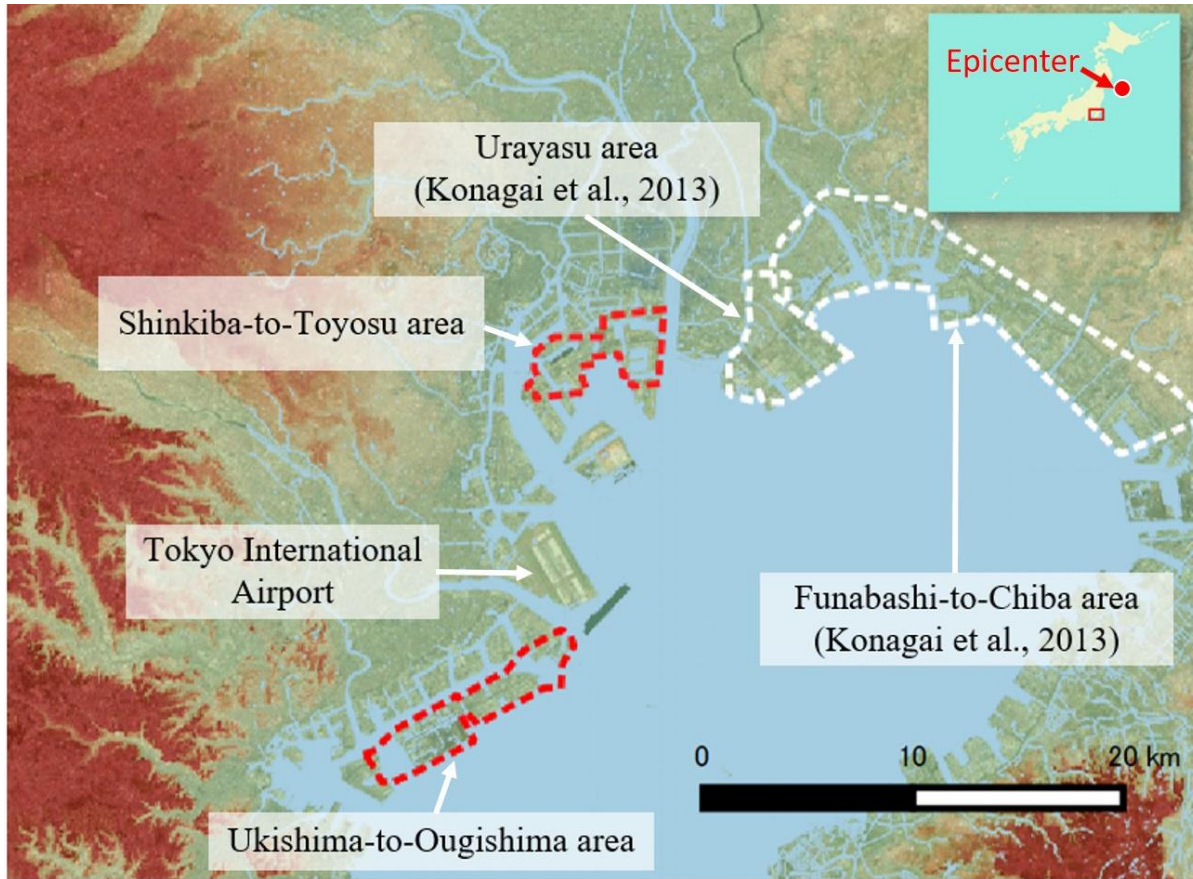


Fig. 1 – Air-borne LiDAR surveyed areas

2. The detection of liquefaction-induced ground subsidence from LiDAR

A Light Detection and Ranging (LiDAR) is a technique for rapid and accurate collection of ground elevation data. It consists of (1) a laser scanner, (2) a kinematic airborne Global Positioning System (GPS), (3) an interfaced Inertial Measurement Unit (IMU), and (4) a fixed, ground-based reference GPS station for detecting difference between its position indicated by satellites and this ground-based reference for correcting positioning errors. In this system, the laser scanner emits fast pulses from focused infrared laser, which are beamed toward the ground surface with an oscillating mirror for fast scanning in a sinusoidal pattern. And the reflection of the pulse is detected by the laser scanner. A kinematic GPS measures the spatial position of the platform aircraft, while the IMU records the pitch, roll, and heading of the aircraft. Using the spatial position of the platform aircraft, constant speed and travelling time of laser, the XYZ coordinates of the laser-shot points on the ground surface can be calculated.

The obtained high-resolution digital elevation maps (Digital Surface Models: DSMs hereafter) before (in 2006 for the entire target area) and after the earthquake (in September 2014 for Ukishima-to-Ougishima area and October 2014 for Shinkiba-to-Toyosu area) are graphic images of pixels having information of their elevations. These images have different spatial pixel densities for different areas and times, depending on the safe flight altitudes allowed for the aircraft to fly near the Tokyo International Airport. The increase in flight altitude can also yield increase of errors because the laser-light beam can spread transversely as it propagates. In general, change in elevation can be easily obtained by comparing DSMs at different times. However, obtained change in elevation includes not only liquefaction-induced ground subsidence but also above-mentioned system-correlated anomalies, the effect of deep-seated tectonic deformations caused by this earthquake which was really remarkable over the entire stretch of the Pacific coast areas of the eastern Japan [3]. To detect liquefaction-induced soil subsidence from LiDAR images, an attempt is made to cancel out these anomalies in accordance with the template matching technic [3].

2.1 Cancelling out of vertical biases

Liquefaction-induced shallow ground subsidence can be simply measured with reference to elevations of top ends of pile supported building and bridge piers such that any potential horizontal or vertical biases can be eventually cancelled out. Therefore, to find the best matching depth for DSMs to minimize the effect of both system-correlated anomalies and the tectonic deformations, template matching technique is used for end-bearing pile-supported buildings chosen as the template in the source image of target areas.

Total 11 points on flat roofs of 10 pile-supported buildings and a road surfaces of viaducts were chosen as template points for the two target areas. In Shinkiba-to-Toyosu area, 7 points on flat roofs of 7 pile-supported buildings and a road surface of pedestrian bridge were taken as templates to find the best matching depth (Fig.2a). At each template point, a circle with radius of 2 to 3 m is drawn around it, and elevations of the DSM points that fall within this circle are averaged for the representative value of the point's elevation. As shown in Fig.3a, the elevations of the chosen points after the earthquake are 8.0cm higher than those before the earthquake in average with the standard error of 0.8cm.

Correspondingly, in Ukishima-to-Ougishima area, 4 points on flat roofs of 3 pile-supported buildings and 2 road surfaces of expressway viaducts were taken as templates to find the best matching depth (Fig.2b). The change in elevation at each template points were measured in the same manner mentioned above. The Ukishima-to-Ougishima area was divided in two sub-areas, west and east of Kawasaki River Channel. As shown in Fig.3b, for the west and east subareas, the elevations of the chosen points after the earthquake are 0.8cm and 10.2cm lower than those before the earthquake in average with the standard error of 1.6cm and 0.35cm, respectively. These standard errors of 0.8cm, 1.6cm and 0.35cm are considered to be small enough to discuss large soil subsidence that appeared as clear as several tens centimeters difference in level between ground floors of pile-supported RC buildings and sidewalks. These values of change in elevation were used to cancel the vertical biases.

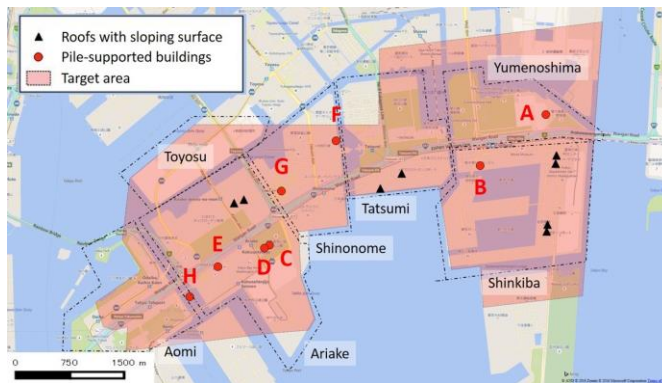


Fig. 2a – Template points in Shinkiba-to-Toyosu area



Fig. 2b – Template points in Ukishima-to-Ougishima

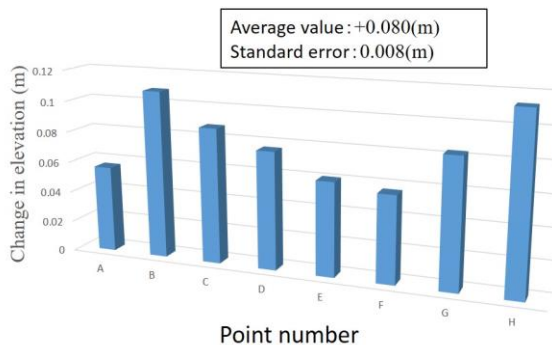


Fig. 3a – Observed vertical biases in Shinkiba-to-Toyosu area

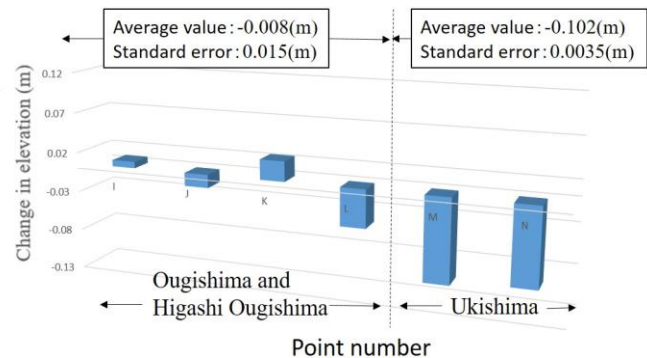


Fig. 3b – Observed vertical biases in Ukishima-to-Ougishima area

2.2 Cancelling out of lateral biases

For cancelling lateral biases, we need to extract Lagrangian components of displacements. However, Comparing DSMs at different times only allows to detect Eulerian ground displacement, in which the description of motion is made in terms of the spatial coordinates which does not follow the motion of a particular target. One method to extract Lagrangian components of displacements is to detect edges of buildings where elevation changes sharply and keep tracking the motion of the detected edges. However, the DSMs have a spatial resolution of 5.2 pixels/m² at most, which is a little sparse for sharp edge detection.

To deal with this problem, Konagai et al. [2] proposed one method to detect lateral Lagrangian displacements from Eulerian displacements of roofs with sloping surfaces towards walls. As illustrated in Fig.4, several cross-sections of a roof are drawn first, and after those with outshooting objects are excluded, they are averaged for the representative roof shape with two sloping surfaces towards walls on both sides.

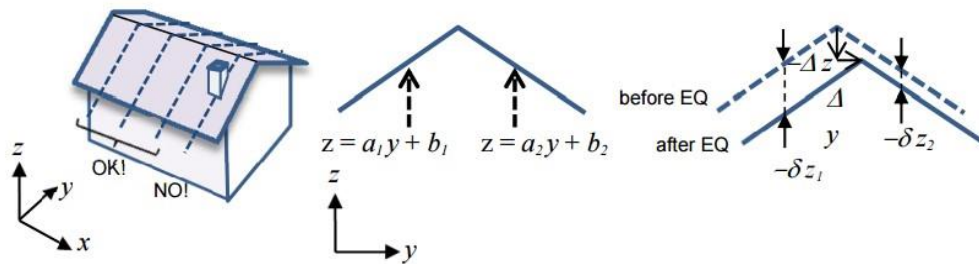


Fig. 4 – Template building with sloping roofs [2]

If a roof undergo a rigid-body-translation movement, the vertical Eulerian displacement of the roof can be divided into two types (Fig.4). Therefore, the lateral Lagrangian components $\{ \Delta y \ \Delta z \}^T$ can be obtained by solving the following simultaneous equations.

$$\begin{Bmatrix} \delta z_1 \\ \delta z_2 \end{Bmatrix} = \begin{bmatrix} -a_1 & 1 \\ -a_2 & 1 \end{bmatrix} \begin{Bmatrix} \Delta y \\ \Delta z \end{Bmatrix} \quad (1)$$

where $\{ \delta z_1 \ \delta z_2 \}^T$ are Eulerian displacements of the two sloping roof surfaces. It is noted that even a pile-supported building may not be an appropriate target for lateral template matching, because piles are laterally flexible enough to be easily deformed by the movements of their surrounding soils.

Therefore, as for Shinkiba-to-Toyosu area, 3 buildings in areas with no evidence of liquefaction are taken as templates though 8 buildings with two sloping roof surfaces are available in this area (Fig.2a). As shown in Fig.5a, the points on a stable ground have shifted about 4.4cm east and 1.5cm south in average with standard deviations of 5.0cm and 9.7cm, respectively. Correspondingly, as for Ougishima area, 3 buildings in areas with no evidence of liquefaction are taken as templates though 8 buildings are available in target area (Fig.2b). As shown in Fig.5b, the points on stable ground have shifted about 4.5cm west and 1.9cm north in average with standard errors of 6.9cm and 8.1cm, respectively. Since the average value of extracted lateral components of Lagrangian displacement for both target areas are at most 4.5cm, lateral biases are considered to be negligible.

It is noted that the DSMs were prepared on new Japanese National Grid System which is named JGD2011. The Japanese National Coordinate System divides Japan into a set of 19 zones assigned with Greek numerals from 1 to 19 in principle in a row-by-row pattern starting from the zone at southwest corner. The surveyed Tokyo Bay area is included in Zone 9 with its northwest corner located at 138.5° E, 36.0° N. Previously used coordinate system which had been used before 2011 was recently updated to JGD2011 with revised coordinates of geodetic control points in East Japan after the Great East Japan Earthquake. Since new Japanese National Grid System was applied to DSMs, lateral components of Lagrangian displacements are considered to be smaller than that of previous study [2].

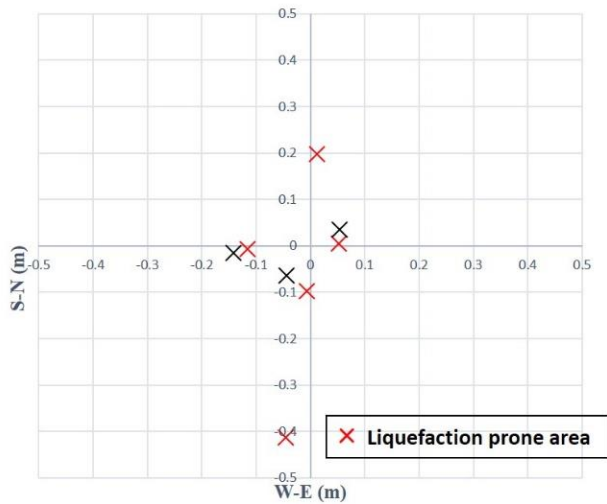


Fig. 5a – Lagrangian components of lateral shifts in Shinkiba-to-Toyosu area

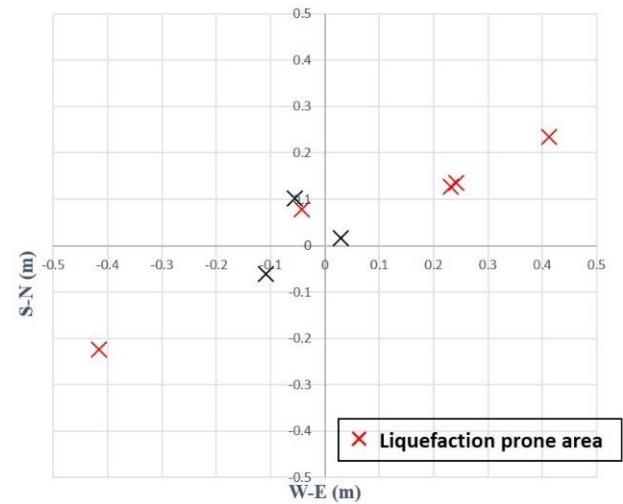


Fig. 5b – Lagrangian components of lateral shifts in Ukishima-to-Ougishima area

3. Obtained subsidence map for the west part of Tokyo Bay shore area

By comparing two DSMs before and after earthquake and subtracting tectonic displacements and anomalies using above-mentioned method, soil subsidence maps were prepared as shown in Fig.6 and Fig.7. These maps cover the Keihin-Industrialized region that encompasses the metropolis of Tokyo and includes the eastern part of Kanagawa prefecture. In these maps, +1.0m and -1.0m were set as upper and lower threshold values of the change in elevation respectively to remove the effect of artificial change of terrain. However, it is noted that some small artificial change of terrain such as road repairing may be included in this map.

3.1 Shinkiba-to-Toyosu Area

Fig.6 shows the obtained soil subsidence map for Shinkiba-to-Toyosu Area. These reclaimed lands have been constructed after around the early 1900s with soils dredged from the bottom of the Tokyo Bay and household solid waste from Tokyo metropolis. The spatial pattern of ground subsidence shown in Fig.6 is consistent as a whole with that described in the damage investigation report of the Japanese Geotechnical Society [4]. Zooming in on a middle of Shinkiba district, a remarkable ground subsidence is found. Aerial photographs [5] [6] on the upper left corner of the figure taken in 1964 and 1971, respectively, shows that the remarkable ground subsidence can be seen where landfilling was made during the period from 1964 to 1971.

3.2 Ukishima-to-Ougishima Area

Fig.7 shows the obtained soil-subsidence map of Ukishima-to-Ougishima area. This area forms a part of Keihin-Industrialized region that encompasses the metropolis of Tokyo and includes the eastern part of Kanagawa prefecture, Japan. This area is formed through a series of reclamation projects, which started around 1950s and development have continued till date. These artificial islands are called Ougishima, Higashi Ougishima and Ukishima from west to east. They are landfills of sand dredged from the bottom of the Tokyo Bay and covered up with sand transported from the Boso Peninsula of Chiba prefecture. On this map, subsidence can be seen over the entire stretch of reclaimed lands. In particular, remarkable subsidence is seen in the middle of Ukishima. Zooming in on one of the industrial complex in Higashi Ougishima, ground subsidence near oil storage tanks is relatively small compared to surrounding ground as shown on upper right of Fig.7. This reduction of ground subsidence is considered to be largely due to liquefaction counter measures such as soil improvement.

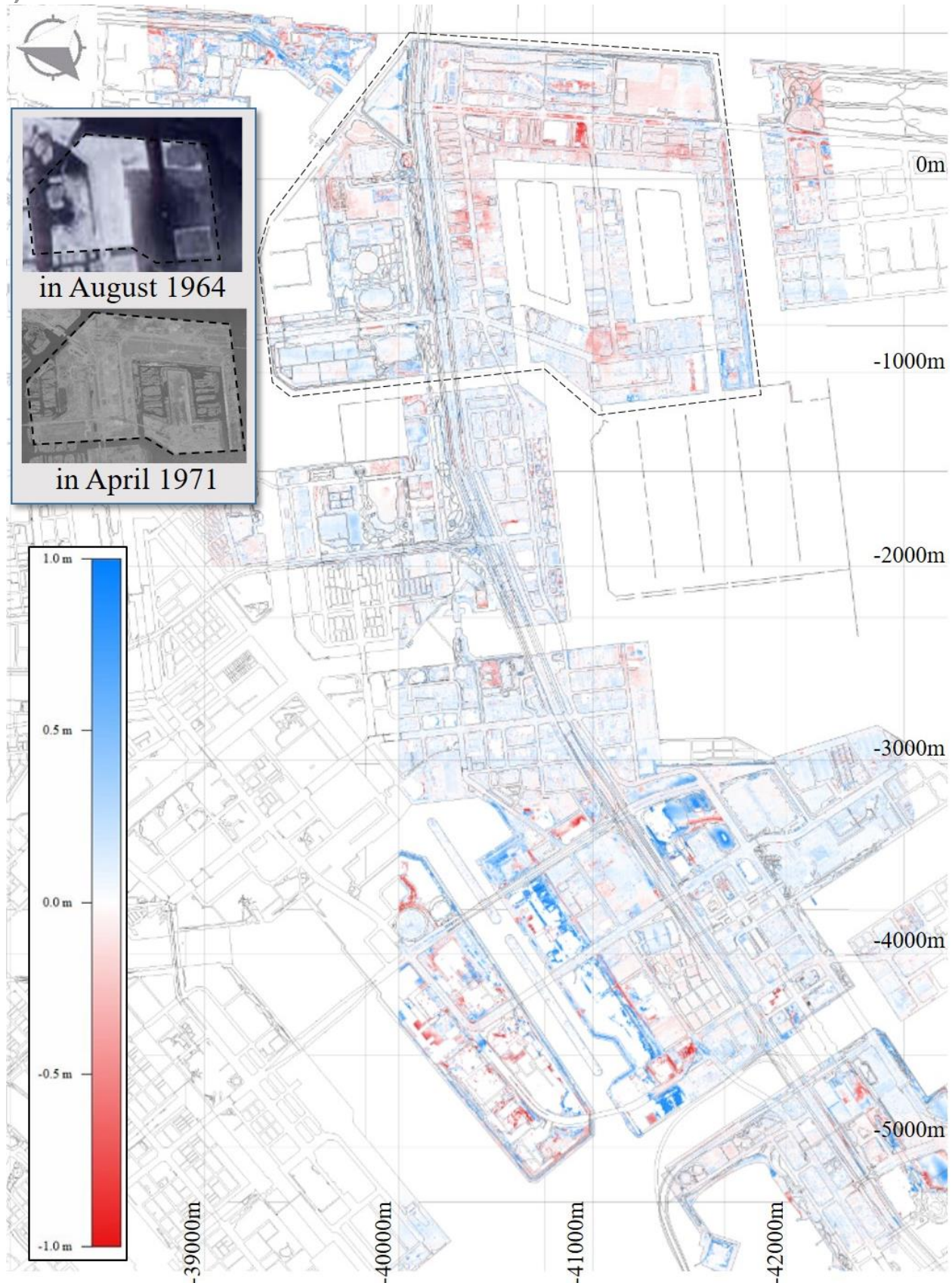


Fig. 6 – Soil subsidence map of Shinkiba-to-Toyosu area (Refer Fig.2a for place names)

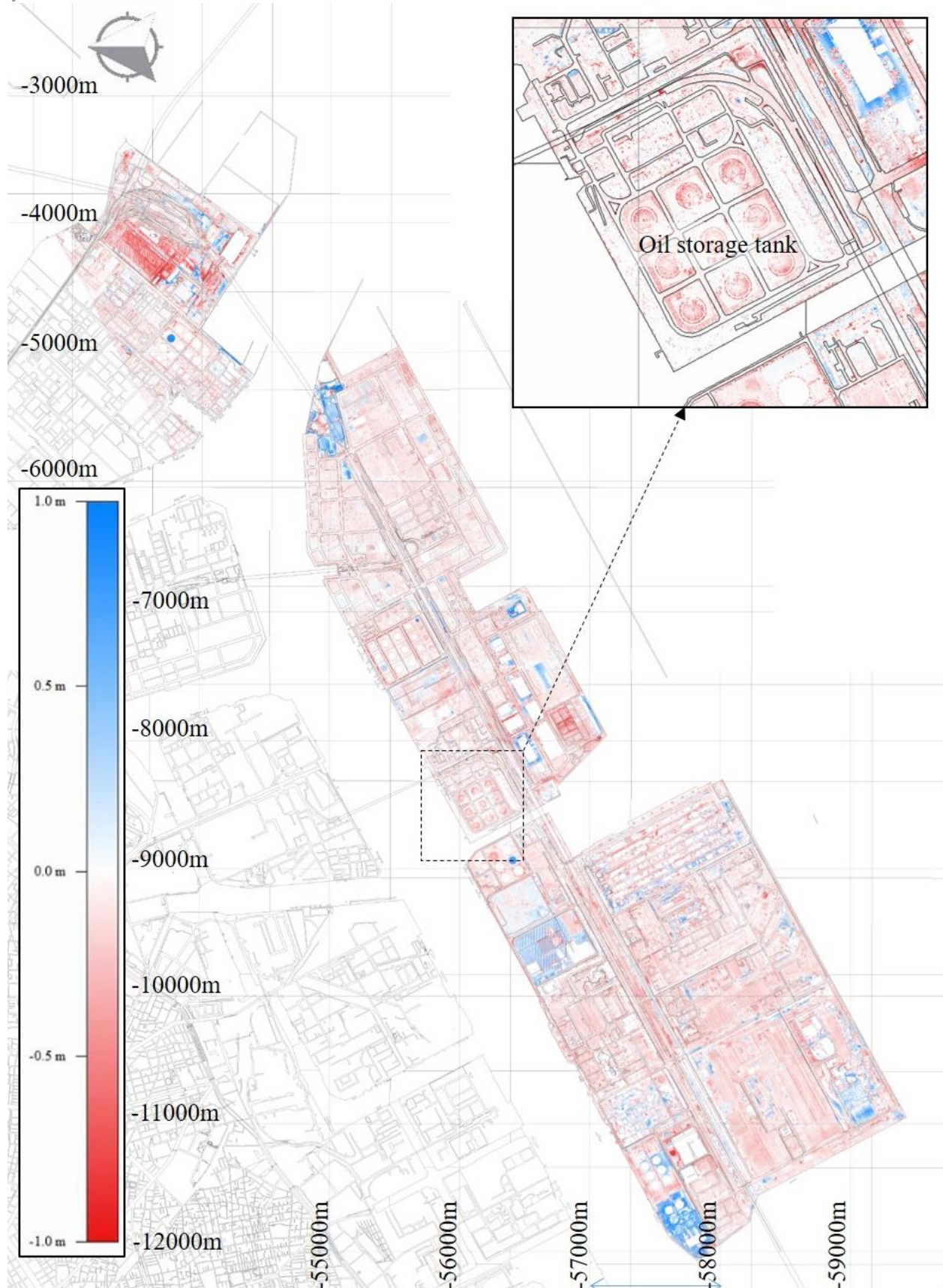


Fig. 7 – Soil subsidence map of Ukishima-to-Ougishima area (Refer Fig.2b for place names)

4. Verification of subsidence map

For verification of subsidence maps, differences in levels between ground floors of pile-supported building and their surrounding sunken ground were measured at 8 locations only in Shinkiba-to-Toyosu Area and compared with those extracted from subsidence map. Soil subsidence at each point was extracted from a circle with radius of 1m drawn near the pile-supported building and averaged for the representative value of ground subsidence. Fig.8 shows both the actual and extracted values of ground subsidence in Shinkiba-to-Toyosu Area. Measured values of ground subsidence are generally in good agreement with those extracted from the subsidence map with the mean value and the standard errors of 0.019m and 0.05m, respectively.

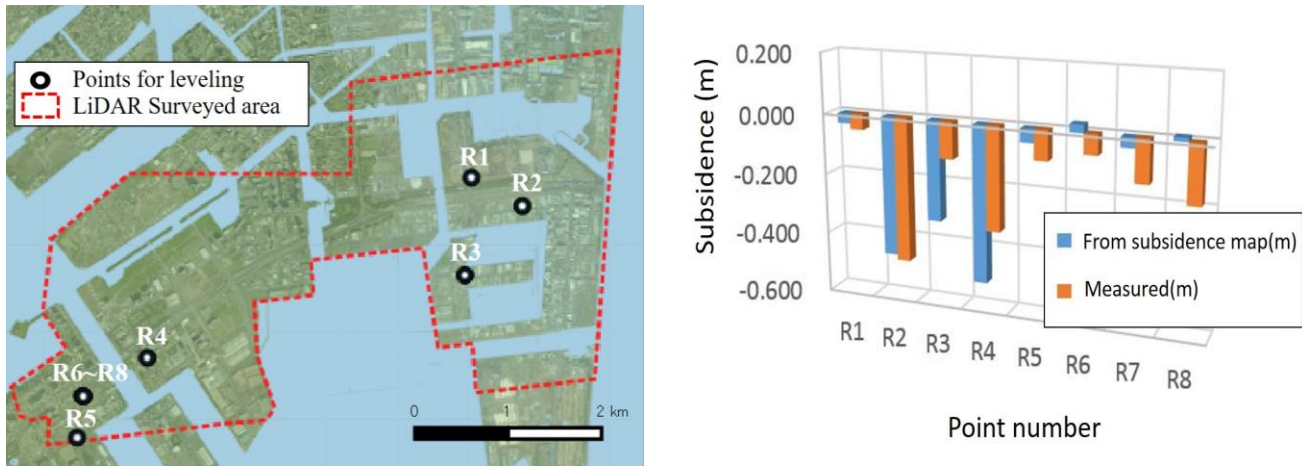


Fig. 8 – Difference in level between ground floors of pile supported buildings and surround sunken sidewalks

5. Conclusion

The March 11th 2011 Great East Japan Earthquake has caused severe liquefaction damage over the entire stretch of reclaimed lands along the coast of the Tokyo Bay. The liquefied areas along the coast of Tokyo Bay reportedly reached 42 km² (Yasuda, 2011), and there yet remain serious long-lasting concerns about sewage treatment, possible inundations inside levees and so on.. In response to this earthquake, Konagai et al (2013) immediately prepared soil subsidence map for the eastern part of the Tokyo Bay Shore area. In this study, soil subsidence map was further extended to cover the west part of the Tokyo Bay, which includes the Keihin-Industrialized region that encompasses the metropolis of Tokyo and includes a coastal part of Kanagawa prefecture, Japan.

To measure liquefaction-induced soil subsidence, two sets of Digital Surface Models (DSMs) before and after the earthquake were first compared with 10 pile-supported buildings and 3 viaducts as template points for matching. Though obtained subsidence map includes the effect of small artificial change of terrain such as road repairing, the spatial pattern of ground subsidence shown in subsidence map is consistent, on the whole, with that described in the damage investigation report. On the obtained subsidence map of Shinkiba-to-Toyosu area, remarkable subsidence can be seen in the places where landfilling was made during the latter half of reclamation project. The subsidence map of Ukishima-to-Ougishima area shows that the ground subsidence near an oil storage tank is relatively small compared with surrounding ground, which may indicates that obtained subsidence map can be used to evaluate the effectiveness of liquefaction counter measures such as soil improvement.

Finally, ground subsidence extracted from the subsidence map was compared with the differences in level between ground floors of pile-supported buildings and the surrounding sunken ground in Shinkiba-to-Toyosu area. Measured values of ground subsidence are generally in good agreement with those extracted from the subsidence map, with the mean value and the standard errors of estimates being 0.019m and 0.05m, respectively. These values are considered to be small enough to discuss large-scale ground subsidence caused by liquefaction, but should be further minimized by increasing the number of reference points used for template matching.



6. Acknowledgements

The Digital Surface Models (DSMs) and subsidence prepared here are one of the results of cooperative survey between Konagai Laboratory, Yokohama National University, Japan and Aero Asahi Corporation, Japan. Aero Asahi Corporation retains copyright control over Digital Surface Models as their works. The authors' deepest appreciation goes to Metropolitan Expressway Company Limited, Japan who has provided the authors with valuable pieces of information about pile-supported highway structures. Special thanks of authors also go to all the members of Konagai Laboratory who kindly supported site investigations for this study.

7. References

- [1] Yasuda, S., Harada, K., Ishikawa, K., Kanemaru, Y. (2012): Characteristics of liquefaction in Tokyo Bay area by the 2011 Great East Japan Earthquake. *Soils and Foundations*, Vol. 52(5): 793-810.
- [2] Konagai, K., Kiyota, T., Suyama, S., Asakura, T., Shibuya, K., Eto, C. (2013): Maps of soil subsidence for Tokyo bay shore areas liquefied in the March 11th, 2011 off the Pacific Coast of Tohoku Earthquake. *Soil Dynamics and Earthquake Engineering*, Vol.53, pp.240-253.
- [3] Geospatial Information Authority of Japan (2011), Crustal movement caused by the March 11th 2011 Off the Pacific Coast of Tohoku Earthquake detected through continuous GPS monitoring, available from (<http://www.gsi.go.jp/chibankansi/chikakukansi40005.html>.)
- [4] Ministry of Land Infrastructure and transportation, Japanese Geotechnical Society (2011): In-depth report of the ground in Kanto region liquefied in the 2011 Tohoku Pacific Earthquake., No.003, No.017, N0.021
- [5] Tokyo Port Musium (2008): History of reclamation project in Tokyo port, available from (https://www.tokyoport.or.jp/43pdf_01.pdf) (in Japanese)
- [6] Geospatial Information Authority of Japan (2015): Achieves of aerial photographs for tracing the history of land, available from: (<http://www.gsi.go.jp/tizu-kutyu.html>). (in Japanese)